MONS HANSTEEN: MORPHOMETRY, PETROGRAPHIC MAPPING, AND MODE OF EMPLACEMENT. R. Evans[1,2], R. Lena[1,3], C. Wöhler[1,4,5], A. Berezhnoy[6]. [1]Geologic Lunar Research (GLR) Group; [2]114 Simonds St., Fitchburg, MA 01420, USA; revans_01420@yahoo.com; [3]Via Cartesio 144, sc. D, I-00137 Rome, Italy; r.lena@sanita.it; [4]Daimler Group Research and Advanced Engineering, D-89013 Ulm, Germany; christian.woehler@daimler.com; [5]Applied Informatics, Faculty of Technology, Bielefeld University, D-33615 Bielefeld, Germany; [6]Sternberg Astronomical Institute, Moscow State University, Moscow, Russia; ber@sai.msu.ru

Introduction: Mons Hansteen is a well-known lunar Red Spot feature in the highlands which has a distinctive arrow-head shape. Lunar Red Spots are dome-like or mound-like high-albedo extrusive features of volcanic origin which display strong absorptions at near-ultraviolet wavelengths. Various Red Spots are described in [1]. Their spectral signatures are different from those of mare basalts but also of the highland areas surrounding them. Among the Red Spots, the highland domes Gruithuisen γ and δ and the nearby Northwest Dome, situated at the border of Mare Imbrium, and the three Mairan domes, located at the eastern border of Sinus Roris, are described as volcanic edifices in [2]. Their formation from highly viscous silicic non-mare lavas in the pre-mare late Imbrian period is discussed in [3]. Detailed mapping of the distribution of non-mare volcanic material is performed in [4] based on Clementine UVVIS data. The rheologic properties of the lavas that formed the Gruithuisen domes are determined quantitatively in [5], and the dimensions of their feeder dikes are estimated. It is demonstrated in [6] that a further Red Spot, situated at the southwestern border of Oceanus Procellarum and termed Hansteen α or Mons Hansteen, is most likely of volcanic origin and was also formed by extrusion of viscous non-mare lavas. Red Spots are different in appearance from lunar mare domes in that the lavas that formed them appear to be much more viscous, and the main contenders are dacitic or rhyolitic lavas [6, 7].

In this study we determine the morpometric properties of Mons Hansteen based on telescopic CCD imagery, estimate the rheologic properties of the dome-forming lava, and perform a petrographic analysis of the dome material using Clementine UVVIS+NIR data.

Stratigraphy of the Hansteen region: It is indicated in [6] that Mons Hansteen is not covered by ejecta of the nearby Imbrian aged craters Hansteen and Billy (which formed 3.8–3.9 Ga ago). Its precise age is not known, but stratigraphic studies and crater counts indicate an age of between 3.74 and 3.6 Ga [8]. The Imbrian impact occurred approximately 3.91 Ga ago. Most lunar Red Spot features are assumed to be Imbrian and to have been active before the filling of the lunar maria in successive flows dating at approximately 3.55 Ga (peak), 3.2–3.3 Ga, and 2.4 Ga ago. Crater counts on the Gruithuisen domes indicate that they formed between 3.85 and 3.7 Ga ago. Stratigraphic studies of the nearby craters Hansteen and Billy indicate ages between 3.8 and 3.9 Ga. Accordingly, no mafic ejecta of these craters are detected on the surface of Mons Hansteen [8].

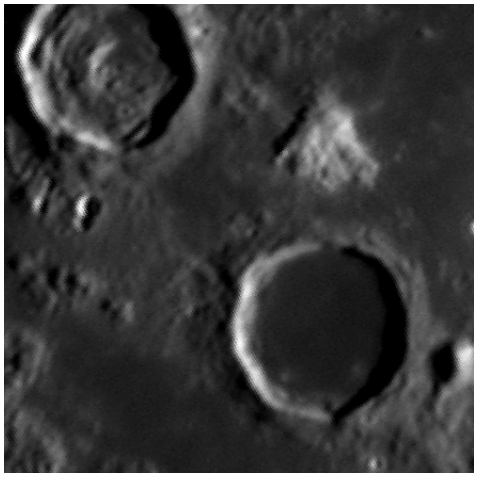

Fig. 1: Telescopic CCD image of Mons Hansteen and the nearby craters Hansteen (upper left) and Billy (lower right), acquired on October 30, 2009, at 21:59 UT.

Morphometric and rheologic properties: Mons Hansteen is roughly triangular in shape with a dimension of 30 km in north-south direction and 25 km in east-west direction. Lunar Orbiter image IV-149-H2 shows a few peaks casting shadows to the west, indicating height differences of about 500–600 m. The lower-sun view of Consolidated Lunar Atlas plate E23 suggests that the main peaks rise about 1000 m above the mare. Our shadow length measurements in the low-sun telescopic CCD image shown in Fig. 1 indicate a height of Mons Hansteen of 810 m and a flank slope of about 3.1°. The approximation of a parabolic dome shape [5] yields an edifice volume of 289 km³. The effusion rate inferred for Mons Hansteen based on the rheologic model introduced in [5] yields an upper limit for the lava viscosity of about 10^8 Pa s under the assumption that it is a monogenetic dome. A formation during several subsequent effusion phases, which is not unlikely due to the rough and strongly textured surface of Mons Hansteen, would imply lava viscosities lower by at least an order of magnitude. For comparison, the lavas that formed the steeper Gruithuisen domes with their flank slopes between 7° and 15° had viscosities around 10^9 Pa s [5].

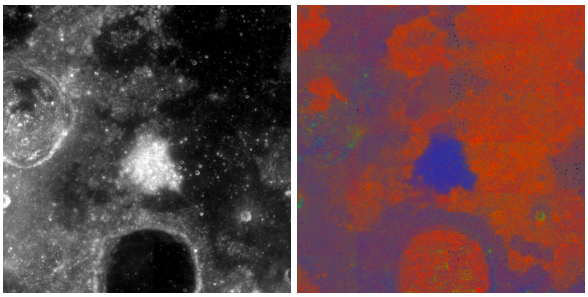

Fig. 2: Left: Clementine 750 nm image of the region around Mons Hansteen. Right: Petrographic map.

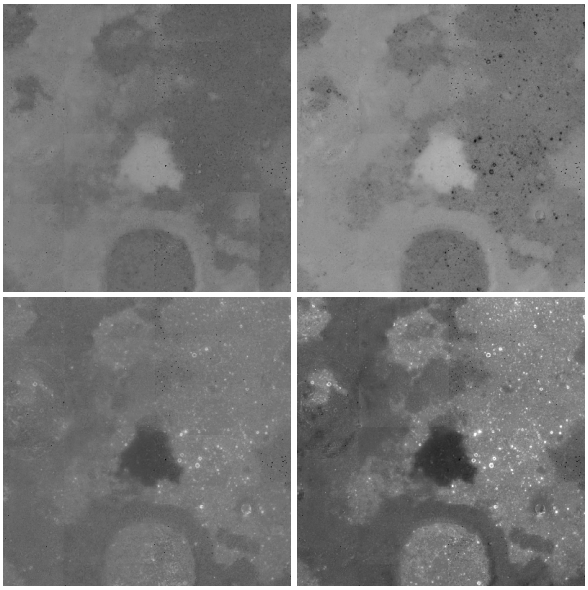

Fig. 3: Elemental abundance maps of (per row, top left to bottom right) Ca (grey value range 2–18 wt%), Al (0–20 wt %), Fe (0–25 wt%), and Mg (0–16 wt%). Spatial resolution is 0.01° (300 m).

Spectral properties: Compared to the Gruithuisen and Mairan domes examined in [5, 9, 10], Mons Hansteen displays a higher albedo at 750 nm (0.2 vs. 0.14–0.18) and a higher $R_{415}/_{750}$ ratio (0.59 vs. 0.54–0.58). Based on Clementine UVVIS+NIR multispectral imagery (www.mapaplanet.org), we furthermore determined the continuum slope of the spectrum, the width of the ferrous absorption trough around 1000 nm, and the wavelengths and relative depths of the individual absorption minima and inflection features [11]. Mons Hansteen displays a single absorption at 1000 nm, indicating the presence of high-Ca clinopyroxene. In contrast, the surface northeast of Mons Hansteen, the complete lava-flooded floor of Billy, and a patch in the northern part of the crater Hansteen are characterised by a shallow pyroxene absorption at 960 nm and a second, deeper absorption at 1190 nm which is presumably due to an admixed olivine component. The region west of Mons Hansteen spectrally appears as a mixture between mare basalt and highland material.

Elemental abundances and petrographic analysis: We estimated the abundances of the elements Ca, Al, Fe, Mg, Ti, and O in the region around Mons Hansteen based on the previously extracted spectral features, mapping them to Lunar Prospector gamma ray spectrometer data using the second-order polynomial regression method introduced in [12]. Furthermore, we determined the petrographic map shown in Fig. 2, which indicates the relative fractions of the three end-members mare basalt (red channel), Mg-rich rock (green channel), and ferroan anorthosite (FAN, blue channel) as proposed in [13]. Mons Hansteen appears as an "island" of highland material (blue) surrounded by mare basalt (red) and a mixture of FAN and mare basalt (purple). The floor of Billy and part of the floor of Hansteen are also covered by mare basalt.

Four elemental abundance maps are shown in Fig. 3. According to Table 1, Mons Hansteen is rich in Ca and Al and poor in Fe, Mg, and Ti. Our Fe and Ti maps are very similar to those obtained with classical approaches based on Clementine UVVIS data [14]. The elemental abundances according to Table 1 correspond to a typical highland soil composition [15]. Similar values were obtained for the Gruithuisen domes .

	Ca	***Al***	***Fe***	***Mg***	***Ti***	***O***
Mons Hansteen	11.3	13.3	5.0	4.5	0.40	44.9
Gruithuisen δ	11.1	13.5	4.3	5.1	0.22	45.1
Gruithuisen γ	10.9	13.3	5.2	4.8	0.45	44.9
Northwest dome	10.8	13.0	5.4	5.0	0.50	44.5

Table 1: Estimated elemental abundances in wt%.

Conclusion: The morphometric and rheologic analysis suggests that Mons Hansteen was formed by the effusion of highly viscous, non-basaltic lavas. The estimated elemental abundances are similar to those inferred for the Gruithuisen domes and confirm that Mons Hansteen consists of highland-like material.

References: [1] Wood and Head (1975), *Conf. Origins of Mare Basalts and Lunar Evolution*; [2] Head and McCord (1978), *Science 199*; [3] Head et al. (1978), *LPSC IX*; [4] Chevrel et al. (1999), *JGR 104(E7)*; [5] Wilson and Head (2003), *JGR 108(E2)*; [6] Hawke et al. (2003), *JGR 108(7)*; [7] Hawke et al. (2002), *Workshop Moon Beyond 2002*; [8] Wagner et al. (2004), *LPSC XXXV*; [9] Wöhler et al. (2006), *Icarus 183*; [10] Lena et al. (2007), *Planet. Space Sci. 55*; [11] Evans et al. (2009), *LPSC XXXX*; [12] Wöhler et al. (2009), *EPSC 2009*; [13] Berezhnoy et al. (2005), *Planet. Space Sci. 53*; [14] Lucey et al. (2000), *JGR 105(E8)*; [15] General Dynamics/Convair Study, http://www.nss.org/settlement/spaceresources/1979-LunarResourcesUtilization2-Results.pdf.